Impact of Ultracapacitor Modelling on Fast Frequency Control Performance

Matej Krpan
Department of Energy and Power Systems
Faculty of Electrical Engineering and Computing
University of Zagreb
Zagreb, Croatia
Email: matej.krpan@fer.hr

Igor Kuzle
Department of Energy and Power Systems
Faculty of Electrical Engineering and Computing
University of Zagreb
Zagreb, Croatia
Email: igor.kuzle@fer.hr

2020 International Conference on Smart Grids and Energy Systems (SGES) | 978-1-7281-8550-7/20/$31.00 ©2020 IEEE | DOI: 10.1109/SGES51519.2020.00064

***Abstract*—This paper explores the impact of ultracapacitor (UC) modelling on fast frequency response performance. The dynamic model of the UC bank is based on the nonlinear dynamic model of the UC cell which takes into account the dependence of the UC parameters on the applied DC voltage. The complete system is modelled and tested on IEEE 39-bus system in DIgSILENT PowerFactory for overfrequency and underfrequency events. The performance of the realistic UC model is compared against an ideal ultracapacitor model to show that the ideal representation is not always appropriate, although for most cases the ideal model will suffice.**

***Index Terms*—frequency control, inertial response, power system dynamics, ultracapacitor, ultracapacitor, virtual inertia, synthetic inertia**

I. Introduction

The trend of increasing inverter-interfaced generation (IIG) in power systems throughout the world and subsequent reduction of synchronous inertia has motivated many research efforts on understanding stability of low-inertia systems as well as developing new algorithms which enable the IIG participation in system frequency control and other ancillary services [1], [2].

In literature, much attention has been given to the application of batteries mainly for frequency control due to their fast response. However, standalone grid-scale UC banks exist that can be used as an alternative to batteries for fast frequency response because they can reach rated power output in milliseconds which is similar to batteries, but they can withstand significantly more charging/discharging cycles (up to millions compared to thousands in batteries) [3], [4]. Furthermore, UC can be charged and discharged to/from full power in a matter of seconds due to high current withstanding capabilities. UC is also complementary to a battery and can be used in coordination to maximize the benefits of both systems.

The work of the authors is a part of the H2020 project CROSSBOW — CROSS BOrder management of variable renewable energies and storage units enabling a transnational Wholesale market (Grant No. 773430). This document has been produced with the financial assistance of the European Union. The contents of this document are the sole responsibility of authors and can under no circumstances be regarded as reflecting the position of the European Union. This work has been supported in part by the Croatian Science Foundation under the project WINDLIPS - WIND energy integration in Low Inertia Power System (grant No. PAR-02-2017-03).

There were many papers utilizing ultracapacitor technology for various applications. Ultracapacitor technology for electric vehicle applications was studied in [5]–[7] in which the focus was on numerical modelling and power electronics control for energy management. UCs are often paired with wind and/or solar generation systems for power smoothing, virtual inertial response or low-voltage ride through (LVRT) [8]–[14] in which the focus was on enhancing existing capabilities of wind/solar generation systems. On larger scale applications, ultracapacitor is often used as a part of a hybrid ESS in microgrids [15]–[17] or isolated power systems [18]–[22] for leveling out intermittent renewables or for grid ancillary services such as frequency or voltage support.

However, almost all of these papers have one thing in common: the ultracapacitor is represented with an ideal capacitor which may not be always appropriate. Research [23]–[25] has shown that the ultracapacitor capacitance varies with the applied voltage. Since the energy stored in a (ultra)capacitor is directly proportional to the voltage, an error may arise when sizing and calculating stored energy for certain application.

There were no papers that investigated the impact of ultracapacitor modelling on its performance for fast frequency control which is the topic of this paper. It should be noted that the findings of this paper are relevant for studies when the UC bank model is based on a capacitor element. On the other hand, simpler models exist, e.g. [26] which are appropriate for integration in bulk power system simulation software. Such models do not model the capacitor behaviour behind the inverter and the performance is controlled based on initial state-of-charge and time integration of power output during simulation.

II. Ultracapacitor bank modelling

The equivalent circuit of a UC cell for fast charging/discharging dynamics is shown in Fig. 1 [23]–[25]. Majority of the ultracapacitor capacitance comes from C_{uc} which is a voltage-dependent capacitance. Voltage-dependent part of this capacitance can range up to 40% of total capacitance at rated voltage based on the cell in question [24], [25]. Series

978-1-7281-8550-7/20/$31.00 ©2020 IEEE
DOI 10.1109/SGES51519.2020.00064

combination of parallel branches $R_1^sC_1^s$–$R_n^sC_n^s$ is actually an infinite series of these parallel groups. However, 5 elements are enough to obtain an accurate model according to [25]. Parameters of the RC circuit are defined by (1)–(3) [25].

$$C_{uc}(u_C) = C_0 + k_v u_C(t) \tag{1}$$

$$C_k^s = \frac{1}{2}C_{uc}, \quad k \in \{1...n\} \tag{2}$$

$$R_k^s = \frac{2\tau(u_C)}{k^2\pi^2 C_{uc}} \tag{3}$$

C_0 is the ultracapacitor capacitance at 0 V and k_v is a constant expressed in F/V. $\tau(u_C)$ is another experimentally determined parameter (it has a dimension of time) and can also be expressed as function changing linearly to the output voltage: $\tau(u_C) = \tau_0 + k_\tau u_C(t)$ [25]. However, it can also be approximated by (4) [25]:

$$\tau(u_C) \approx 3C_{uc}(R_{dc} - R_s), \tag{4}$$

where R_{dc} is the equivalent series resistance experimentally obtained at very low frequencies (essentially DC). Naturally, $R_{dc} > R_s$. All these parameters can be identified using manufacturer's data sheet.

A. Impact of ultracapacitor modelling level of detail

Simulations of different model responses are conducted in MATLAB-Simulink using *Simscape Electrical* toolbox. Dedicated models of a commercial ultracapacitor [25] was used with varying levels of detail to show the differences in performance. Input to the model is the current $i_{uc}(t)$ and output of the model is the ultracapacitor voltage $u_{uc}(t)$. Results are shown in Fig 2. Firstly, it can be seen that the parallel groups do not play a significant impact in the voltage response (Fig. 2a). Generally, accuracy of voltage response is not lost if the parallel groups are neglected, although at least one should be included if greater accuracy is to be achieved since the difference in stored energy estimation can be up to 10% on average due to losses.

Fig. 2b shows that using the ideal capacitor representation may yield inaccurate voltage response. In this case, the most accurate response was achieved with capacitance at half the rated voltage. However, this may not always be the case as the expression for C_{uc} also plays a role. Nevertheless, the ideal representation will not reflect the voltage transient effect which occurs when the charging or discharging current is discontinued due to the ESR effect. Fig. 2c shows the difference between stored energy for a detailed model and an ideal capacitor. If ideal capacitor representation has to be used, than it is better to use a capacitance value which is closer to the ultracapacitor capacitance at between half the rated voltage and capacitance at 0 V because the error in stored energy is significantly smaller. Generally, the value of stored energy will be more optimistic for an ideal model than for nonideal model.

Energy in an ideal ultracapacitor and energy in a nonideal ultracapacitor are described by equations (5) and (6), respectively. Energy in the two models is equal when the capacitance

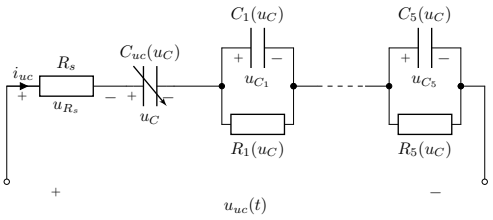

Fig. 1. Detailed RC circuit of an ultracapacitor cell

of the ideal model is set to (7). Obviously, the ideal model exactly represents the energy stored in a nonideal model only for a certain operating point (voltage).

$$E_{ideal} = \int_0^U C \cdot u \cdot du = \frac{1}{2}C_{ideal}U^2 \tag{5}$$

$$E_{real} = \int_0^U (C_0 + k \cdot u) \cdot u \cdot du = \frac{1}{2}C_0U^2 + \frac{1}{3}kU^3 \tag{6}$$

$$E_{ideal} = E_{real} \Leftrightarrow C_{ideal} = C_0 + \frac{2}{3}kU. \tag{7}$$

B. Scaling up the cell model to form a bank

A single ultracapacitor cell, although it can have a large capacitance in thousands of Farads, is too small to provide any significant power output since it is only rated up to a few Volts. Therefore, a certain number of cells must be connected in series (n_s) to form a string of higher voltage. Then, a certain number of strings must be connected in parallel n_p to achieve larger capacitance and higher current rating. Equivalent capacitance and resistance of a system is equal to (8)–(9), respectively. To form a grid-scale ultracapacitor bank (1–100+ MW), this means hundreds to thousands of cells in series and tens to hundreds of strings in parallel.

$$C_{sys} = C_{cell}\frac{n_p}{n_s}. \tag{8}$$

$$R_{sys} = R_{cell}\frac{n_s}{n_p}. \tag{9}$$

The dynamic model of the UC bank in the time domain is developed by setting $u_{uc}(t)$ as an output $y(t)$, $i_{uc}(t)$ as an input $u(t)$. Capacitor voltages are chosen as state variables. Complete nonlinear model of the ultracapacitor bank in the analytic form is described by (10)–(15) where R_k^s and C_k^s are defined by (2) and (3), respectively.

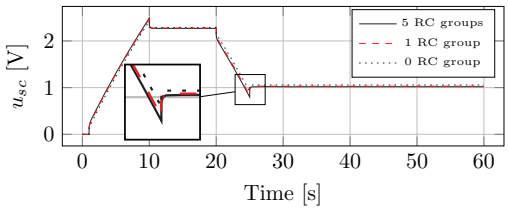

(a) Voltage response to different numbers of RC groups

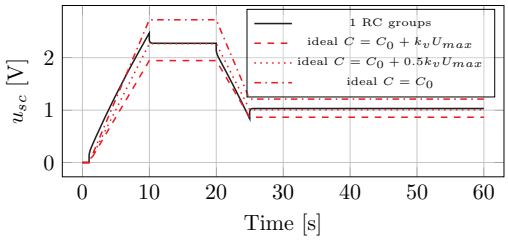

(b) Voltage response compared to ideal capacitor

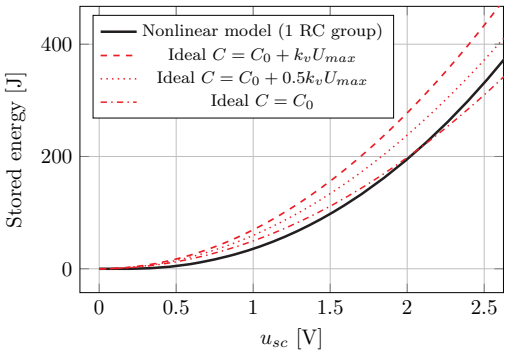

(c) Energy stored in an ultracapacitor with respect to voltage

Fig. 2. Maxwel BCAP0140 model response for different number of parallel RC groups in the first branch and comparison to the ideal capacitor representation

$$u_{uc}(t) = i_{uc}(t)R_s + u_C(t) + \sum_{k=1}^{n} u_{C_k^s} = y(t) \tag{10}$$

$$i_{uc}(t) = u(t) \tag{11}$$

$$u_{uc}^s(t) = n_s u_{uc}(t) = n_s y(t) \tag{12}$$

$$i_{uc}^m(t) = n_p i_{uc}(t) = n_p u(t) \tag{13}$$

$$\frac{du_C}{dt} = \frac{i_{uc}(t)}{C_0 + k_v u_C(t)} \tag{14}$$

$$\frac{du_{C_k^s}}{dt} = -\frac{u_{C_k^s}}{R_k^s C_k^s} + \frac{i_{uc}(t)}{C_k} \tag{15}$$

Complete block diagram of the ultracapacitor bank model described by (10)–(15) is shown in Fig. 3.

III. Control System

The complete system with controls is shown in Fig. 4. P and Q are active and reactive power injected or absorbed by the inverter to or from the grid, while asterisk (*) denotes a set-point value. V_{ac}^{grid} is the AC voltage of the bus the inverter is connected to. i_d and i_q are the direct and quadrature axis currents of the inverter. Inverter is controlled in the grid voltage reference frame. PLL estimates the grid voltage angle as well as the frequency for frequency control block. DC current calculation block calculates the UC current for charging or discharging. PQ control, PLL and inverter modules are all standard elements found in many generic IIG models [27].

A. Charge control

Fig. 5 shows the structure of this block. State-of-Voltage (SoV) measurement is used to control the charging and discharging process since the energy of an UC is directly proportional to voltage. Charging is stopped if the UC module is charged to nominal voltage, while discharging is stopped when the ultracapacitor voltage falls below a user defined minimum voltage threshold. Charging/discharging is enabled again when the voltage reaches a user defined minimum voltage level for charging/discharging.

B. DC current calculation

Input to the ultracapacitor model is the current, thus this block calculates the charging or discharging DC current based on the actual inverter power output. Block diagram of this subsystem is shown in Fig. 6. $I_{ch}^{\max}$ and $I_{dch}^{\max}$ are the maximum string charging and discharging current. Note that the module operates in constant power output. Even though a UC can be operated from 0 to rated voltage, for constant power output this will not be possible since for very low voltage, a very high current would be needed which could be more than rated current. Therefore, for constant power control, minimum voltage limit is set according to the maximum current limit or other system limitation (e.g. DC-DC converter limitations). Up to 75% of rated UC energy can be extracted between half the rated voltage and rated voltage [28].

C. Frequency control module

Frequency control loop is shown in Fig. 7. The input to this block is the grid frequency signal estimated by the PLL and the output is the requested change in power. A standard virtual inertia control (washout filter) used in many grid-following converter based systems is implemented in this paper (e.g. wind power [2], [29]).

IV. Simulation and Results

The performance of the proposed model is tested on a modified IEEE 39-bus 10-machine New England test system (inertia of G01 was reduced from 5 s to 1 s on 10000 MVA base to simulate a reduced inertia system and G10 hydro turbine was replaced with a faster IEEE GAST turbine model with default parameters). A 500 MVA ultracapacitor bank is connected to Bus 14. It consists of 4000 cells in series and 500 of those strings in parallel with the cell capacitance equal to $C_{uc} = 800 + 100u_C(t)$ Farads. For this ultracapacitor cell, the voltage-dependent part of the capacitance is around 25% of total capacitance at rated voltage (2.5 V) which is a realistic number for commercial cells (which can range from 10% to

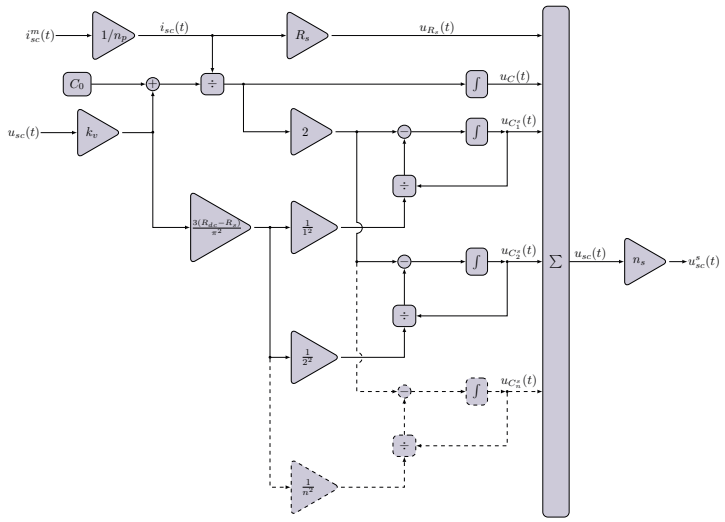

Fig. 3. Block diagram of the nonlinear ultracapacitor bank

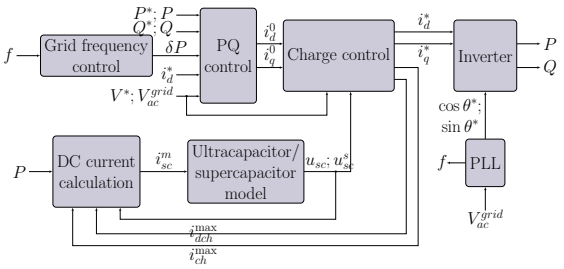

Fig. 4. Complete model of the UC bank system

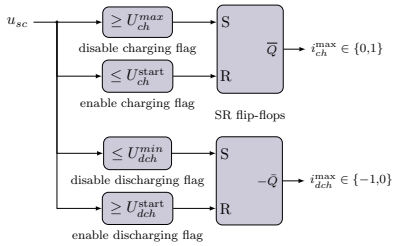

Fig. 5. Charge control

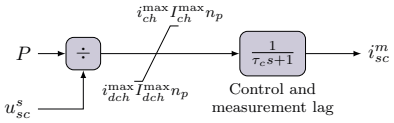

Fig. 6. DC current calculation block

45% based on [24], [25], [30] and datasheets of commercial UC cells). Rest of the UC bank parameters are given in the Appendix. RMS simulations (10 ms time step) have been conducted in DIgSILENT PowerFactory.

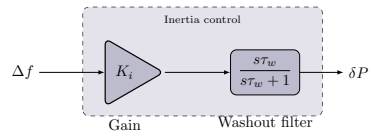

Fig. 7. UC bank grid frequency control module

A. Underfrequency event

At $t = 1$ s, generator G05 initially operating with 254 MW is tripped to trigger an underfrequency event. Figure 8 shows that for a fully charged ultracapacitor the ideal and nonideal model behave exactly the same regardless of the size of the voltage dependent part of capacitance. However, for a partially discharged UC (in this case, 60% of rated voltage), the calculated frequency response is visibly different depending on the choice of the ideal model capacitance, i.e. in this case the error in frequency nadir ranges between 0.03 Hz and 0.1 Hz which is a large enough difference between triggering underfrequency load shedding or not. However, the range over which the ideal model accurately describes the realistic behaviour may be smaller if the voltage-dependent capacitance is bigger or if the contingency is bigger. If ideal capacitor representation is used, then its capacitance should be chosen somewhere between the capacitance at 0 V and capacitance at half the rated voltage depending on the operating point and the expression for UC capacitance. The difference in performance will always arise when the ultracapacitor is completely discharged. This is because of the difference in stored energy as each model will stop discharging at different time. In terms of frequency control, this means that they will stop discharging at different output power which will cause different (secondary) frequency nadir. Nonetheless, for most underfrequency contingency simulations, the UC will be fully charged so the ideal model is applicable.

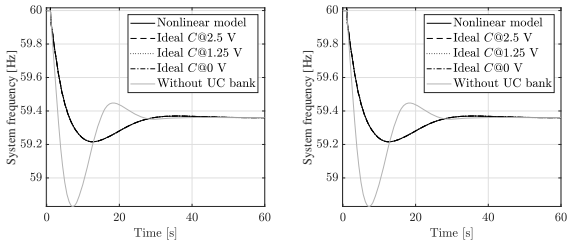

(a) $C_{uc} = 800 + 100u_C$; $C_0/C_{max} \approx 0.75$ (b) $C_{uc} = 900 + 60u_C$; $C_0/C_{max} \approx 0.85$

Fig. 8. Frequency response for an ultracapacitor charged to rated voltage

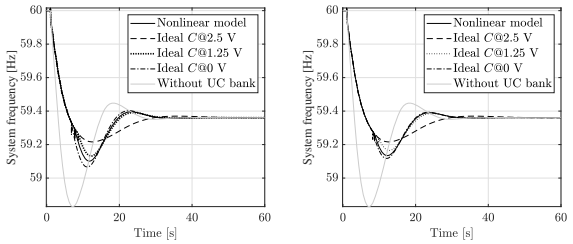

(a) $C_{uc} = 800 + 100u_C$; $C_0/C_{max} \approx 0.75$ (b) $C_{uc} = 900 + 60u_C$; $C_0/C_{max} \approx 0.85$

Fig. 9. Frequency response for an ultracapacitor charged to 60% of rated voltage

B. Overfrequency event

At $t = 1$ s, 628 MW load at Bus 20 is tripped to trigger an overfrequency event. The behaviour is expected to be similar to the behaviour during underfrequency event, although complementary. In other words, since the overfrequency event mandates that the UC bank will be charged instead of discharged, then the major difference in model performance is expected near full charge which is the worst case scenario. Fig. 10 shows that the differences in model performance are visible but they are not significant (difference in frequency is around 0.01 Hz) for all ideal representations meaning that the ideal model accurately describes the realistic model. For smaller initial SoC, there is no difference between an ideal and realistic model.

C. Internal dynamics of an ultracapacitor

Fig. 11 shows the UC bank voltage and power profile for the underfrequency event case from Section IV-A for the UC model $C_{uc} = 800 + 100u_C$. Fig. 11a and Fig. 11b shows that the ultracapacitor will discharge with different rates depending on the modelling and value of the capacitance (as well as initial voltage).

For a fully charged UC, different models will end up with different state of voltage after the inertial response, i.e. they will have different energy stored. In this case, the ideal capacitor with rated capacitance (@2.5 V) will have the most accurate voltage profile. However, there is no difference in power profile (Fig. 11c) because the voltage profile is between

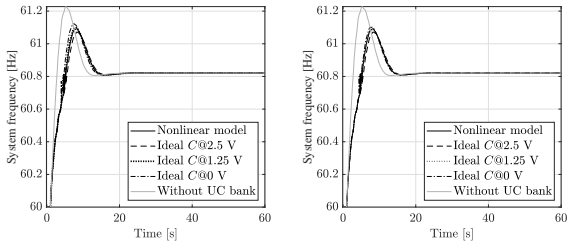

(a) $C_{uc} = 800 + 100u_C$; $C_0/C_{max} \approx 0.75$ (b) $C_{uc} = 900 + 60u_C$; $C_0/C_{max} \approx 0.85$

Fig. 10. Frequency response to an overfrequency event for an ultracapacitor charged to 95% of rated voltage

the minimum and maximum limits for all models. Therefore, the requested power output will be equally delivered by all models.

On the other hand, for an initially partially discharged UC (Fig. 11b), different models will hit the minimum voltage limit at different times, i.e. the output power profile will be discontinued at different points. In other words, this acts as another disturbance of different magnitude hence the system frequency response will be different. In this case, the ideal model with capacitance at 0 V reached the minimum voltage limit while still discharging 100 MW to the grid. On the other hand, the ideal model with rated capacitance had enough energy to sustain the requested power profile. Nevertheless, the secondary frequency drop can be avoided by switching to constant current mode or using energy-estimation based control [26].

V. Conclusion

In this paper we have investigated the impact of ultracapacitor modelling on its performance in fast frequency control.

The capacitance of the ultracapacitor varies with cell voltage and an equivalent series resistance exists which is neglected in ideal capacitor model usually used in literature to represent the ultracapacitor. We have shown that the ideal model can represent the realistic ultracapacitor in terms of energy stored only in a single operating point in steady-state (i.e. capacitor voltage). Generally, the ideal model with minimum ultracapacitor capacitance will yield accurate enough results in terms of stored energy at a various operating points.

In dynamic simulations for frequency control, the ideal representation is appropriate most of the time. This is when the requested energy from the ultracapacitor is less than the energy stored in the ultracapacitor system. In this case, the response of the ideal model is the same as the response of the nonlinear model. However, since different models with different capacitance values will discharge at different rates, the ideal representation may not adequately represent the realistic behaviour if the requested energy is bigger than the energy stored in the ultracapacitor system. This can lead to erroneous conclusion about the expected frequency response. The range over which the ideal model adequately represents

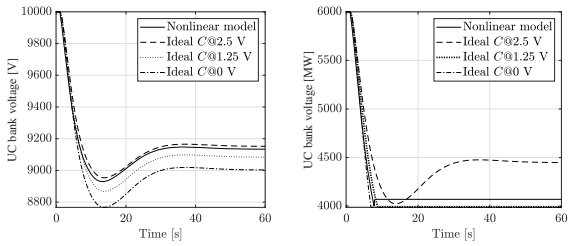

(a) Initial voltage equals to rated voltage

(b) Initial voltage equals to 60% rated voltage

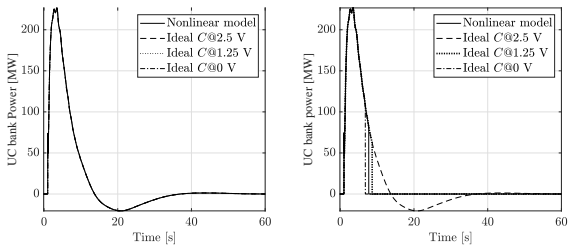

(c) Power profile for fully charged UC

(d) Power profile for 60% rated voltage

Fig. 11. UC bank voltage and power profile for two different initial voltages

the realistic model depends on the size of the contingency and the ultracapacitor control system.

APPENDIX

Ultracapacitor bank system parameters: n_s = 4000, n_p = 500, bank rated power: 500 MW, $C_0 = 800/900$ F, $k_v = 100/60$ F/V, $R_{dc} = 0.5$ mΩ, $R_s = 0.25$ mΩ, $I_{ch}^{\max}/I_{dch}^{\max} = \pm 250$ A, $U_{ch}^{\max} = 2.51$ V, $U_{ch}^{\text{start}} = 2.25$ V, $U_{dch}^{\min} = 1$ V, $U_{dch}^{\text{start}} = 1.25$ V, $\tau_c = 50$ ms, $K_i = 200$ p.u., $\tau_w = 1$ s, $K_p^d = K_p^q = 1$ p.u., $K_i^d = K_i^q = 100$ p.u.

REFERENCES

[1] F. Milano, F. Dörfler *et al.*, "Foundations and challenges of low-inertia systems (invited paper)," in *2018 Power Systems Computation Conference (PSCC)*, June 2018, pp. 1–25, doi: 10.23919/PSCC.2018.8450880.

[2] M. Krpan and I. Kuzle, "Dynamic characteristics of virtual inertial response provision by dfig-based wind turbines," *Electr. Power Syst. Res.*, vol. 178, p. 106005, 2020.

[3] X. Luo, J. Wang *et al.*, "Overview of current development in electrical energy storage technologies and the application potential in power system operation," *Applied Energy*, vol. 137, pp. 511–536, jan 2015.

[4] Maxwell Technologies, "Ultracapacitors frequency response application brief," 2018, technical brochure.

[5] L. H. Saw, H. M. Poon *et al.*, "Numerical modeling of hybrid supercapacitor battery energy storage system for electric vehicles," *Energy Procedia*, vol. 158, pp. 2750 – 2755, 2019.

[6] L. Li, Z. Huang *et al.*, "A rapid cell voltage balancing scheme for supercapacitor based energy storage systems for urban rail vehicles," *Electr. Power Syst. Res.*, vol. 142, pp. 329 – 340, 2017.

[7] A. Tahri, H. E. Fadil *et al.*, "Management of fuel cell power and supercapacitor state-of-charge for electric vehicles," *Electr. Power Syst. Res.*, vol. 160, pp. 89 – 98, 2018.

[8] T. Zhou and W. Sun, "Optimization of battery–supercapacitor hybrid energy storage station in wind/solar generation system," *IEEE Transactions on Sustainable Energy*, vol. 5, no. 2, pp. 408–415, April 2014.

[9] L. Qu and W. Qiao, "Constant power control of dfig wind turbines with supercapacitor energy storage," *IEEE Trans. Ind. Appl.*, vol. 47, no. 1, pp. 359–367, Jan 2011.

[10] W. Li, G. Joos, and J. Belanger, "Real-time simulation of a wind turbine generator coupled with a battery supercapacitor energy storage system," *IEEE Transactions on Industrial Electronics*, vol. 57, no. 4, pp. 1137–1145, April 2010.

[11] M. F. M. Arani and E. F. El-Saadany, "Implementing virtual inertia in dfig-based wind power generation," *IEEE Trans. Power Syst.*, vol. 28, no. 2, pp. 1373–1384, May 2013.

[12] M. Krpan and I. Kuzle, "Coordinated control of an ultracapacitor bank and a variable-speed wind turbine generator for inertial response provision during low and above rated wind speeds," in *2019 IEEE Sustainable Power and Energy Conference (iSPEC)*, Nov 2019, pp. 1693–1698.

[13] S. I. Gkavanoudis and C. S. Demoulias, "A combined fault ride-through and power smoothing control method for full-converter wind turbines employing supercapacitor energy storage system," *Electr. Power Syst. Res.*, vol. 106, pp. 62 – 72, 2014.

[14] J. Fang, Y. Tang *et al.*, "A battery/ultracapacitor hybrid energy storage system for implementing the power management of virtual synchronous generators," *IEEE Trans. Power Electron.*, vol. 33, no. 4, pp. 2820–2824, April 2018.

[15] M. H. Fini and M. E. H. Golshan, "Determining optimal virtual inertia and frequency control parameters to preserve the frequency stability in islanded microgrids with high penetration of renewables," *Electr. Power Syst. Res.*, vol. 154, pp. 13 – 22, 2018.

[16] B. Wang, L. Xian *et al.*, "Hybrid energy storage system using bidirectional single-inductor multiple-port converter with model predictive control in dc microgrids," *Electr. Power Syst. Res.*, vol. 173, pp. 38 – 47, 2019.

[17] L. Yang, Z. Hu *et al.*, "Adjustable virtual inertia control of supercapacitors in pv-based ac microgrid cluster," *Electr. Power Syst. Res.*, vol. 173, pp. 71 – 85, 2019.

[18] J. Kim, V. Gevorgian *et al.*, "Supercapacitor to provide ancillary services with control coordination," *IEEE Trans. Ind. Appl.*, vol. 55, no. 5, pp. 5119–5127, Sep. 2019.

[19] L. Sigrist, I. Egido *et al.*, "Sizing and controller setting of ultracapacitors for frequency stability enhancement of small isolated power systems," *IEEE Trans. Power Syst.*, vol. 30, no. 4, pp. 2130–2138, July 2015.

[20] J. Cao, W. Du *et al.*, "Optimal sizing and control strategies for hybrid storage system as limited by grid frequency deviations," *IEEE Trans. Power Syst.*, vol. 33, no. 5, pp. 5486–5495, Sep. 2018.

[21] Y. Liu, W. Du *et al.*, "Sizing a hybrid energy storage system for maintaining power balance of an isolated system with high penetration of wind generation," *IEEE Trans. Power Syst.*, vol. 31, no. 4, pp. 3267–3275, July 2016.

[22] M. G. Molina and P. E. Mercado, "Modeling of a DSTATCOM with ultra-capacitor energy storage for power distribution system applications," in *XIII Eriac Décimo Tercer Encuentro Regional Iberoamericano de CIGRÉ*, May 2009, pp. 1–8.

[23] S. Buller, E. Karden *et al.*, "Modeling the dynamic behavior of supercapacitors using impedance spectroscopy," *IEEE Trans. Ind. Appl.*, vol. 38, no. 6, pp. 1622–1626, Nov 2002.

[24] R. Faranda, M. Gallina, and D. T. Son, "A new simplified model of double-layer capacitors," in *2007 International Conference on Clean Electrical Power*, May 2007, pp. 706–710.

[25] V. Musolino, L. Piegari, and E. Tironi, "New full-frequency-range supercapacitor model with easy identification procedure," *IEEE Trans. Ind. Electron.*, vol. 60, no. 1, pp. 112–120, Jan 2013.

[26] I. Egido, L. Sigrist *et al.*, "An ultra-capacitor for frequency stability enhancement in small-isolated power systems: Models, simulation and field tests," *Applied Energy*, vol. 137, pp. 670 – 676, 2015.

[27] DIgSILENT GmbH, "Battery energy storing system template," 2017, template documentation.

[28] Maxwell Technologies, "Design considerations for ultracapacitors," 2009, white paper.

[29] M. Krpan and I. Kuzle, "Introducing low-order system frequency response modelling of a future power system with high penetration of wind power plants with frequency support capabilities," *IET Renewable Power Generation*, vol. 12, pp. 1453–1461, October 2018.

[30] E. Tironi and V. Musolino, "Supercapacitor characterization in power electronic applications: Proposal of a new model," in *2009 International Conference on Clean Electrical Power*, 2009, pp. 376–382.